

Multi-faceted particle pumps drive carbon sequestration in the ocean

Philip W. Boyd^{1*}, Hervé Claustre^{2,6}, Marina Levy^{3,6}, David A. Siegel^{4,6} & Thomas Weber^{5,6}

The ocean's ability to sequester carbon away from the atmosphere exerts an important control on global climate. The biological pump drives carbon storage in the deep ocean and is thought to function via gravitational settling of organic particles from surface waters. However, the settling flux alone is often insufficient to balance mesopelagic carbon budgets or to meet the demands of subsurface biota. Here we review additional biological and physical mechanisms that inject suspended and sinking particles to depth. We propose that these 'particle injection pumps' probably sequester as much carbon as the gravitational pump, helping to close the carbon budget and motivating further investigation into their environmental control.

Open ocean waters store (sequester) carbon out of contact with the atmosphere on decadal to millennial timescales; this exerts a major control on global climate by regulating the partial pressure of atmospheric carbon dioxide (P_{CO_2})¹. The magnitude of ocean carbon storage is governed by two well established mechanisms that maintain a surface-to-deep ocean gradient of dissolved inorganic carbon (DIC)—the biological pump and the solubility pump^{2,3}. The solubility pump delivers cold, dense, DIC-rich waters to depth mostly at high latitudes, whereas the biological pump globally exports particulate organic carbon (POC) from surface waters. POC export is largely attributed to the gravitational settling of a subset of the particle assemblage^{1,4}—a process we refer to as the biological gravitational pump (BGP).

The BGP is the key link between upper-ocean photosynthetic carbon fixation, the sustenance of mid-water biota, and carbon storage in the interior of the oceans^{4,5}. It is thought to account for around 90% of the vertical DIC gradient, while the solubility pump explains the remainder¹. In the absence of the BGP, models predict that atmospheric P_{CO_2} would be nearly twofold higher⁶. Contemporary and paleoceanographic observations both reveal that carbon sequestration by the BGP is affected by environmental changes in light, temperature, stratification and nutrient availability^{7,8}, and can itself drive pronounced climate shifts such as glacial–interglacial cycles⁸. Future climate projections suggest that the functioning of the BGP will be altered by global oceanic changes^{7,9}, and could potentially contribute to anthropogenic climate warming via a positive feedback mechanism¹⁰. As a consequence, quantification of the functioning of the BGP requires a reliable baseline of accurate measurements.

The underlying principles of the BGP have long been established¹¹: organic particles are continually produced and recycled in sunlit surface waters, and a small fraction of these settle into the interior of the oceans. The strength of the BGP is often quantified as the rate of particle 'export' from the euphotic zone, the surface mixed layer, or across an arbitrary horizon at 100 m (ref. ¹²). As they sink, particles undergo myriad transformations that lead to a pronounced vertical attenuation of the particle flux; this is often described as a power-law relationship referred to as the 'Martin curve'¹³. The efficiency of the BGP is defined here as the time that exported carbon is kept sequestered from the atmosphere within the

interior of the oceans. It is driven by the depth scale of flux attenuation and by pathways of ocean circulation that carry remineralized carbon dioxide back to the surface¹⁴. Carbon is sequestered for longer than a year by particles that penetrate the permanent pycnocline (beneath the wintertime mixed layer), and for up to centuries by particles that reach deep water masses (generally greater than 1,000 m). Together, the strength and efficiency of the BGP determine the total quantity of carbon that is sequestered biologically in the interior of the oceans.

Recently, analyses of global and regional ocean carbon budgets have identified conspicuous imbalances (that is, two- to threefold less storage) when BGP export fluxes are compared with those derived from geochemical tracers^{15,16}. Such discrepancies highlight the need to reassess the pathways that contribute to carbon storage. Furthermore, rates of site-specific particle export seem to be insufficient to meet the carbon demand of mid-water life (termed mesopelagic biota) by two- to threefold^{17–20}, but in one study this can be balanced using community respiration¹⁸. There is considerable debate over the reasons for these carbon deficits, ranging from biases inherent in observational technologies^{17,21} to the potential role of other mechanisms that deliver carbon (dissolved and/or particulate) to deep waters^{16,22,23}. Traditionally, the biogeochemical functioning of the BGP has been evaluated from quasi one-dimensional (1D) observations of particle flux (Box 1), and extrapolated using Earth system models (ESMs; parameterized with observations^{24–26}) and/or remote-sensing observations²⁶. This approach cannot capture more complex mechanisms of carbon export that are highly variable in space and time (Box 1), which potentially results in the reported carbon budget deficits.

Several lines of research have revealed the importance of additional export pathways that inject particles to depth, termed here particle-injection pumps (PIPs)^{23,27–30}. These can be physically mediated (for example, subduction) and/or biologically mediated (for example, by large mesopelagic migrators), and can potentially export all classes of particle.

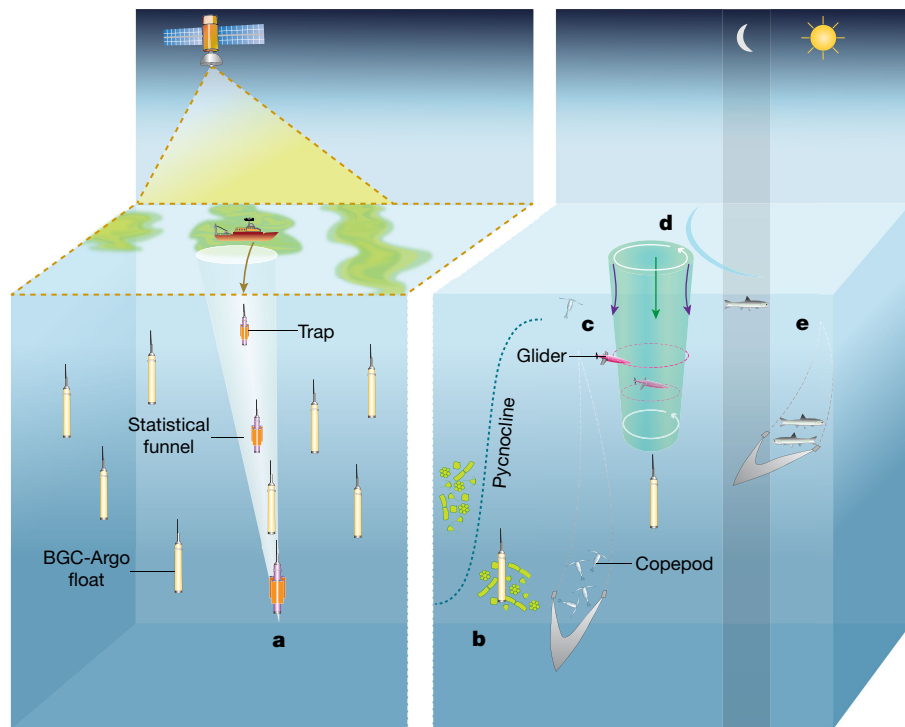
To depth, thus challenging the conventional view of gravitational sinking as the dominant downward pathway for particles into the interior of the oceans. The characteristics of PIPs fundamentally change our understanding of biological carbon sequestration. First, PIPs can animate particle transport spatially into three dimensions (3D), in contrast with the BGP in which the vertical dimension is predominant (1D); second,

¹Institute for Marine and Antarctic Studies, University of Tasmania, Hobart, Tasmania, Australia. ²Sorbonne Université & CNRS, Laboratoire d'Océanographie de Villefranche-sur-mer (LOV), Villefranche-sur-Mer, France. ³Sorbonne Université, LOCEAN-IPSL, CNRS/IRD/MNHN, Paris, France. ⁴Department of Geography and Earth Research Institute, University of California, Santa Barbara, Santa Barbara, CA, USA. ⁵Department of Earth and Environmental Sciences, University of Rochester, Rochester, NY, USA. ⁶These authors contributed equally: Hervé Claustre, Marina Levy, David A. Siegel, Thomas Weber. *e-mail: philip.boyd@utas.edu.au

Box 1

Investigation of downward particle export

The biological gravitational pump (BGP) has traditionally been studied at selected ocean sites using a range of particle interception techniques such as sediment traps (deep-moored, surface-tethered free-drifting, or neutrally buoyant). In the past decade, new tools—including gliders and profiling floats with biogeochemical and bio-optical sensors (BGC-Argo)—have greatly increased the sampling frequency of particle fields in the mesopelagic region of the ocean. Over this period there has also been an upsurge of interest in studying the wide range of mesopelagic fauna using bioacoustics and trawling approaches. Together, these diverse approaches are providing improved estimates of carbon sequestration.



Box 1 Fig. 1 | Approaches used to investigate downward particle export, from the BGP to PIPs. **a**, The BGP is quantified in a biologically patchy upper ocean (green filaments) using ship-based surface sampling (particle production) and subsurface particle interception by sediment traps, most recently neutrally buoyant traps downstream of particle source regions (orange instruments). This coupled surface–subsurface sampling strategy is logistically complex, temporally and spatially restricted (represented here by a ‘statistical funnel’^{92,93}), and hence provides a ‘1D’ view of particle export that is extrapolated to the basin scale using satellite observations and/or modelling. This 1D viewpoint cannot measure the PIPs presented in **b** to **e**, and is contrasted in **a** with the 4D view^{29,94} obtained by an ensemble of BGC-Argo floats (white instruments). **b**, The mixed-layer pump, in which particles are detrained when the pycnocline (blue dashed line) shallows, can be addressed regionally through backscattering (a proxy for POC) profiles measured by BGC-Argo floats³⁶, or globally using satellite surface-ocean

backscattering and Argo/BGC-Argo (density/backscattering) vertical profiles³². **c**, The seasonal lipid pump can be quantified using surveys of overwintering copepods at depths below the permanent pycnocline and subsequent scaling of their lipid-enriched biomass in carbon content³³. **d**, The eddy-subduction pump can be quantified using gliders (pink instruments) and subsequent modelling³¹, BGC-Argo floats (bio-optics, oxygen, physics)⁹⁴ or surveys based on multiple POC profiles in conjunction with coupled models (regional circulation/particle dynamics)^{30,49}. **e**, The quantification of the mesopelagic-migrant pump (active diel transport of carbon by mid-water biota, denoted by moon and sun symbols) requires mid-water trawl surveys along with metabolic modelling^{54,55}. Some multidisciplinary studies^{30,31,49} have combined these approaches to cross-compare export flux from the BGP (green arrows in **d**) and the eddy-subduction pump (purple arrows represent subsurface particle maxima recorded at the eddy periphery³¹). We note that the large-scale subduction pump²³ is not presented here.

global estimates of PIP carbon fluxes are comparable to those for the BGP^{27,28}; and third, these mechanisms cannot be readily quantified using the traditional toolbox applied to investigate the BGP (Box 1). Overall, the PIPs will increase the strength of the biological pump beyond estimates based on gravitational flux alone, and can change its efficiency by altering the depth of carbon export.

The fate of exported carbon after its delivery to depth has also proven to be more complex and heterogeneous than previously recognized. Particle flux attenuation is now known to vary systematically in space^{14,31,32} and time³³, suggesting that the traditional empirical view¹³ must be replaced by a mechanistic one that considers particle composition and architecture, microbial metabolism, and transformation processes¹⁷.

Together, these developments stand to reshape our understanding of particle transport and remineralization in the interior of the oceans. Here,

for open ocean systems, we review the mechanisms, rates and depths of particle injection by each PIP; the potential for each mechanism to close observed deficits in ocean carbon budgets; and the corresponding remineralization depths of exported POC in the deep ocean. We finish by outlining future research directions needed to combine these developments into a new mechanistic, four-dimensional (4D) view of carbon export and sequestration. This Review does not detail the important role of dissolved organic carbon subduction^{22,23}, nor does it cover the dark microbial carbon pump³⁴ or chemolithotrophy³⁵, which have been reviewed elsewhere (Supplementary Table 1).

Particle injection pump mechanisms

PIPs differ in their mechanisms, temporal scales, spatial scales (Figs. 1, 2a) and geographical extent, but they have common features: they can act

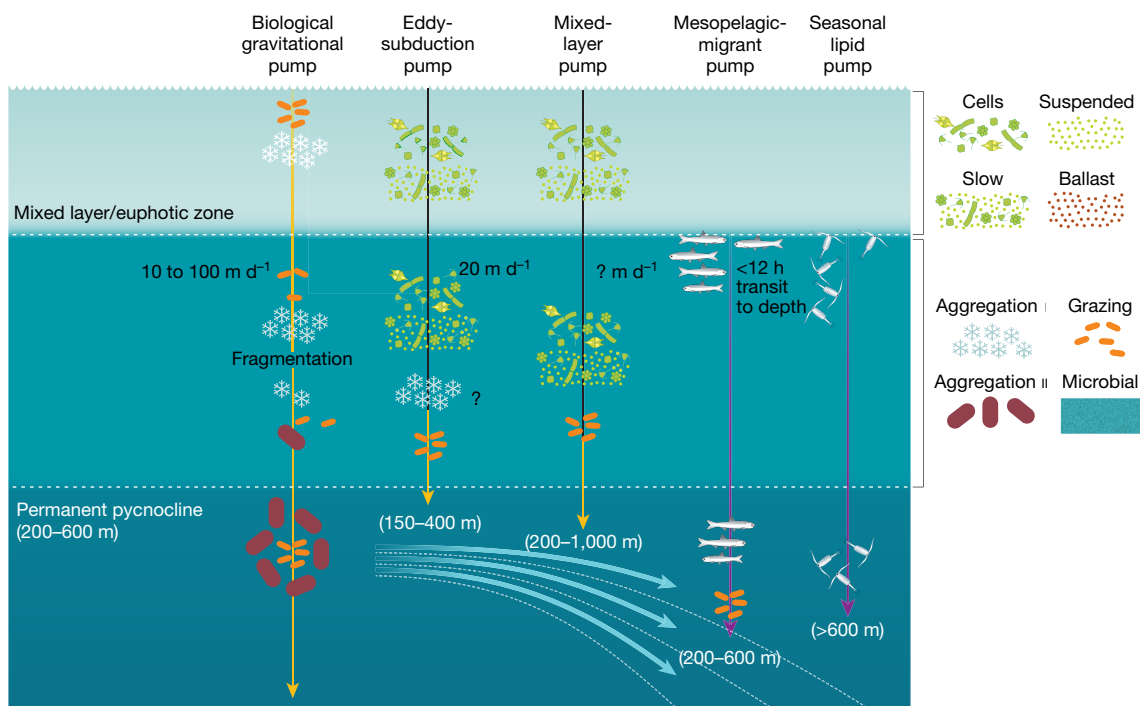


Fig. 1 | Interplay between particle characteristics, mode of export (BGP or PIP), delivery depth and larger-scale ocean circulation for a range of pumps. In the upper layer, the box at the top right represents mixed-layer particle types, which either form large sinking particles (that is, within the BGP; such as faecal pellets and marine snow) or are injected to depth (that is, by PIPs; such as suspended and/or slow-settling heterogeneous particles and cells (including healthy, slow-sinking phytoplankton⁸⁹)). The vertical yellow arrow signifies the BGP; black lines indicate physically mediated PIPs; and purple lines indicate biologically mediated PIPs. The delivery rates of particles to subsurface strata (in m d^{-1} ; ? denotes not known) are presented for each pump. Patchiness in the distribution of vertically migrating animals (top right) has a role in driving three-dimensional particle delivery to depth^{90,91}, and is denoted by different fish or copepod stocks in the upper ocean. The box to the right of the middle layer presents different particle transformations that are central to the BGP¹²;

on all particles, from those that are suspended to those that are sinking (Fig. 1); they typically inject particles below the euphotic zone (that is, the export depth for the BGP), potentially reaching depths of greater than 1,000 m^{28–30} depending on the injection mechanism (Figs. 1, 2b); they occur concurrently with the BGP, but cannot be measured with techniques developed to quantify gravitational settling^{13,32} (Box 1); and their dynamic nature (that is, physical transport^{23,27,28} or patchiness of animal distributions³⁰) means that the interplay between their vertical and horizontal vectors and temporal scales varies considerably (Fig. 1). As such, a 4D sampling framework is required to constrain PIPs (Box 1). The main characteristics of each PIP are elucidated below.

Particle export driven by physical subduction includes several processes that drive the vertical transport of near-surface particles and act on different spatial scales and timescales: subduction caused by mixed-layer shallowing (termed the mixed-layer pump^{29,36}); subduction by large-scale (100–1,000 km) circulation (termed the large-scale subduction pump)²³; and subduction by mesoscale (10–100 km) to submesoscale (1–10 km) frontal circulation (termed the eddy-subduction pump^{23,27,28}).

Carbon export by the mixed-layer pump is driven by biological accumulation of particles throughout the spring and summer growth season; the particles are then diluted to the depth of the mixed layer during winter, and left in the interior of the oceans during early spring stratification (Box 1). This pump operates on wide-ranging timescales—from days or weeks³⁷ to seasons^{29,37}—predominantly in mid and high latitude regions that are characterized by strong seasonal variability in mixed-layer depth (Fig. 2a). Although these concepts are

however, their role is as yet unknown for PIPs. They include microbial solubilization (throughout the water column), aggregation (marine snow denoted by aggregation I; heterogeneous faecally dominated aggregates denoted by aggregation II) and/or disaggregation¹⁸ to form and/or break down heterogeneous particles. In the lower layer, depths in parentheses are the reported delivery depths, with the BGP (and some PIPs) exporting some particles to the sea floor. Blue curved arrows represent the transport of subsurface material along downward-sloping isopycnals (white dashed lines). Major unknowns include whether physical transport by PIPs can cause particle aggregation (signified by ? in the middle section; this is applicable for both subduction and mixed-layer pumps) and hence alter their mode of injection towards gravitational settling (that is, the BGP). Other unknowns include the potential ballasting role of small mineral particles such as aerosol dust for PIPs.

long-established³⁶, only recently have they been scrutinized in detail using advances in optical profiling (BGC-Argo) floats and satellite particle proxies to track particle accumulation rates in relation to changes in surface mixed-layer depth (Box 1).

The large-scale subduction pump is a 3D advective mechanism that transports particles from the seasonal mixed-layer into the interior of the oceans, driven by Ekman pumping and horizontal circulation across a sloping mixed-layer³⁸. Subduction rates were first estimated for the North Atlantic³⁹, and then estimated globally using data-assimilating models⁴⁰. The wide-ranging subduction rates ($1–100 \text{ m yr}^{-1}$)^{39,40} are small relative to particle-settling rates of the BGP^{11,12}; however, subduction occurs over large regions of the global ocean, which boosts the magnitude of carbon delivery to depth.

The frontal-associated eddy-subduction pump subducts particle-rich surface waters on timescales of days and across spatial scales of 1–10 km, driven by strong vertical circulation associated with fronts and eddies^{27,28,41–44}. Gliders are now used to map 3D dynamic eddying flow fields (Box 1), and have found that high particle stocks (that is, co-located POC and chlorophyll indicative of viable phytoplankton) from the spring bloom penetrate the interior of the oceans, and are visible as distinct filaments at depths of 100–350 m at the eddy periphery²⁸ (Box 1). Mapping revealed the co-location of high POC filaments and negative vorticity to depths near the permanent pycnocline²⁸, and the mechanism is supported by high-resolution simulations in which eddy subduction of particles is a recurring feature^{45–48}. The strength of the eddy-subduction pump is governed by the vigour and penetration of the

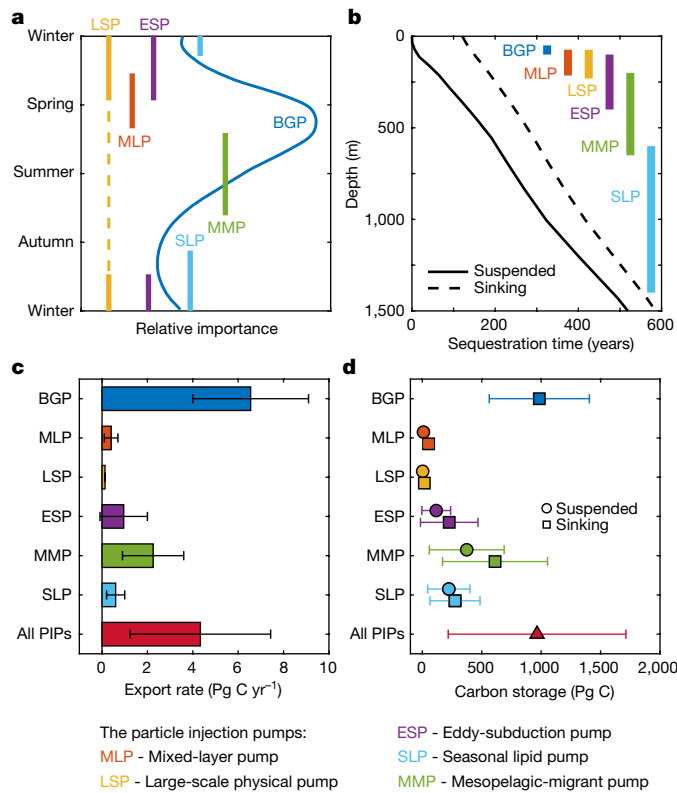


Fig. 2 | Carbon export and storage by PIPs compared to the BGP. **a**, Idealized seasonality of the PIPs for regions that exhibit strong seasonality, where a spring bloom dominates carbon export by the BGP (dark blue line). Coloured bars indicate the season of peak carbon export by the PIPs. We note that the large-scale physical pump should be strongest when mixed layers are deepest, but is probably operative all year (dashed line). ESP, eddy-subduction pump; LSP, large-scale physical pump; MLP, mixed-layer pump; mesopelagic-migrant pump; SLP, seasonal lipid pump. **b**, Sequestration efficiency of the PIPs. Black lines represent the global-mean sequestration timescale for carbon injected at a given depth, defined as the time for remineralized carbon to circulate back to the ocean surface, computed in a data-constrained circulation model (see Supplementary Methods). The solid line assumes that particles are suspended, so remineralization occurs at the injection depth, whereas the dashed line assumes that particles are sinking and remineralize over depth (see Methods). Coloured bars show the injection depth range of the BGP and the PIPs. The efficiency of each pump is defined as the sequestration time from its injection depth. **c**, Strength of the pump mechanisms, defined as their rate of carbon export or injection (see Supplementary Table 1). 'All PIPs' refers to the sum of the five individual PIPs. **d**, Ocean carbon storage by each pump, defined as the product of the strength (c) and efficiency (b). Two scenarios are shown for each PIP, using the sequestration time for suspended (circles) and sinking (squares) particles, whereas the BGP is assumed to export only sinking particles. For the sum of PIPs, we present a 'most likely' scenario, in which the migrant pump injects sinking particles (faecal pellets), and all other PIPs inject suspended particles (triangle).

vertical circulation, in conjunction with local POC stocks over the frontal area^{27,49}. Eddy-subduction rates span $1-100 \text{ m d}^{-1}$ (compared with a range of 20 to more than 100 m d^{-1} for the BGP^{11,12}) depending on the eddy or frontal structure. Modelling indicates that particles subducted by the eddy-subduction pump are remineralized more rapidly (that is, at shallower depths) relative to gravitationally sinking particles²⁷.

The concept of the mesopelagic-migrant pump is based on long-established observations of diurnal vertical migration⁵⁰ (Box 1). This pump extends the remineralization scale by injecting particles to greater depth before decomposition begins^{51,52}, as determined by the gut-retention time of migrating animals⁵¹⁻⁵³ and the depth of their migration (typically around 400 m)⁵³. The injected particles are zooplankton faecal pellets with sinking rates of tens to hundreds of

metres per day⁵¹; compared with loosely packed organic aggregates settling from the surface, these pellets have a faster sinking rate^{11,12} and will penetrate deeper in the water column before remineralization. The mesopelagic-migrant pump therefore influences all important facets of the particle flux that govern carbon sequestration —total export rate, depth of peak flux, and the depth scale of flux attenuation.

Diurnal vertical migration results in active subsurface transport and carbon sequestration; it is usually reported for mesozooplankton and is often included in estimates of the BGP⁵¹. However, vertical migration by larger mesopelagic carnivorous organisms (from greater daytime depths than mesozooplankton) is not sampled by conventional BGP approaches^{52,54}. Targeted studies (Box 1) have quantified that this pump is driven by large mesopelagic migrant carnivores in the Pacific⁵⁴ and in other regions (Supplementary Table 1). The underlying mechanism is upward migration to graze mesozooplankton⁵⁴ followed by rapid (hours) downward migration⁵³—with respiration (release of CO_2), exudation, and defaecation (release of POC/DOC)^{51,55} at depths as deep as 600 m (Box 1), often below that of the permanent pycnocline⁵⁶.

Trawl surveys suggest that approximately 50% of mesopelagic organisms migrate, with this value ranging regionally between 20% and 90% depending on temperature, turbidity and oxygen concentrations^{54,56}. Carbon sequestration by mesopelagic migration is governed by the metabolic transfer efficiency of migrants, and particles are injected at their residence depth; this is often at the upper boundary of oxygen minimum zones where their respiration intensifies oxygen depletion⁵³.

Active transport by vertically migrating metazoans can also occur on longer timescales (Box 1). For example, in high-latitude regions the hibernation of copepods (members of the mesozooplankton) at depths between 600 m and 1,400 m gives rise to a so-called 'seasonal lipid pump'³⁰: during winter hibernation, copepods catabolize carbon-rich lipids that they accumulated in the upper layers during summer; in doing so, they shunt carbon (but not nitrogen and phosphorus) below the permanent pycnocline³⁰. The strength of the seasonal lipid pump is governed by mesopelagic temperature along with the abundance and size of copepods; together, these factors control their respiration rate and help to explain the existence of carbon flux hotspots (that is, patchiness)³⁰.

Another vertical export mechanism that operates on seasonal-migration timescales is zooplankton mortality at their hibernation depth, particularly in high-latitude regions^{57,58}, which sequesters carbon at depths of greater than 500 m. Global extrapolation of seasonal-lipid-pump fluxes, along with the over-wintering mortality flux, is problematic owing to difficulties in sampling and generalizing across distinct regional mechanisms³⁰ (Supplementary Table 1).

The potential for double accounting

The export flux from the BGP is mediated by sinking particles, whereas PIPs can provide additional pathways for all particle classes—from suspended to sinking—to exit the surface ocean (Fig. 1). Thus, there is potential overlap between particles that are delivered from the surface ocean to depth via the BGP and by injection from PIPs. Such overlap—which here is termed 'double-accounting'—may occur when particles associated with the BGP and a PIP are difficult to distinguish and hence could be attributed to more than one pump (Fig. 1). At depth, transformations such as aggregation alter the characteristics of particles, including their size and sinking rate, and hence particles injected by the PIPs can join the sinking flux that is usually attributed to the BGP (Fig. 1). A further factor that introduces overlap between the BGP and PIPs results from the inclusion—for historical reasons⁵⁹—of one component of the mesopelagic migration pump (diurnal migration by mesozooplankton) into the 1D sampling framework of the BGP, while other components (for example, patchier diurnal migration by larger mesopelagic carnivores⁵) are not included. As such, double-accounting can confound our understanding of the relative importance of PIPs to carbon storage in the oceans.

Whether or not it is possible to tease apart the impacts of the individual PIPs is an important question. Forty years of studying the BGP has uncovered a complex biogeochemical system that has multiple drivers and distinguishing characteristics^{11,60}. This body of research helps to frame the differences and similarities between particles delivered to depth by PIPs and those settling via the BGP. Each PIP is distinct with respect to its combination of the type of injected particle (suspended cells to faecal pellets of large mesopelagic migrants), the timing and depth of injection (Fig. 2a, b), and associated particle transformations (aggregation or disaggregation)^{11,12,61}. Additionally, the subsurface ‘fate’ of particles (that is, where they remineralize)—which determines the longevity of carbon sequestration—is driven by the complex interplay between these properties and transformations^{12,60,61}; the composition and architecture of particles determine their sinking speed, whereas myriad processes that are biologically mediated (by microbes and/or zooplankton) and physically mediated (by fragmentation or disaggregation)^{12,62–64} decompose and repackage them over depth (Fig. 1). Therefore, particle fate provides another avenue by which to distinguish the contributions of PIPs from those of the BGP.

So far, evidence of the subsurface fate of injected particles has been largely indirect^{27,28,49}. Surveys of eddy-subduction pumps suggest that injected particles may be remineralized at depths of less than 200 m, based on ammonium peaks⁴⁹, time-series of biogeochemical gradients²⁸, or particle modelling studies²⁷. In the northeast Atlantic, the reported high rates of particle remineralization (from glider-based biogeochemical gradients) must be reconciled with concurrent evidence of coincident, coherent chlorophyll plumes at depths of greater than 300 m, which are indicative of subducted viable phytoplankton²⁸. This glider-based time-series reveals pronounced patchiness²⁸, which suggest that inference of the fate of injected particles—even from state-of-the-art observations—is challenging.

Better constraining of the contribution of each PIP to mesopelagic carbon budgets will require characterization of the injected particle assemblage and their transformations during downwards transport^{12,65–68}. Particle aggregation in PIPs may be driven by convergence or subduction^{69,70} and differential sinking^{65,67}, potentially leading to altered modes of subsurface transport (Fig. 1). BGC-Argo profile observations enable quantification of the size, type, seasonal succession and penetration depths of particles injected by the mixed-layer pump³⁶—properties that have the potential to differentiate them from fast-sinking particles (that is, those transported by the BGP), the distinctive ‘spiky’ bio-optical signature of which is readily detected using multiple sensors⁷¹ (Supplementary Figs. 2, 3). Advances in bio-optics are already making ambiguous signatures associated with slow-sinking particles and zooplankton vertical migration less opaque, lessening the possibility of double-accounting. Such double-accounting may be avoided through the identification of unique characteristics of pumps—including their seasonality (Fig. 2a) or their distinctive regional features³⁰—or through multivariate oceanographic diagnostics⁷².

Carbon sequestration potential

The potential carbon sequestration by each PIP can be quantified as the product of their carbon-injection rate and their sequestration timescale; that is, the time until remineralized carbon is returned to the surface (Supplementary Methods). This timescale is determined both by the injection depth of particles and by their eventual fate; that is, the degree to which they sink or circulate through the ocean before remineralizing to CO₂. In general, deeper particle injection and rapid sinking translates to longer carbon sequestration, because the ‘passage time’ from the ocean interior to the surface increases with depth (Fig. 2b). Here we assemble previous estimates of carbon injection rate and depth (Supplementary Table 1)—along with new modelling projections (Fig. 2)—to estimate carbon sequestration by each PIP, and assess the significance of the PIPs relative to the BGP.

Some targeted studies provide concurrent estimates of carbon injection by individual PIPs and the BGP^{27,28}, whereas others^{30,54,57,58}

facilitate comparison of regional-scale PIP fluxes with independent estimates of the BGP. Both approaches show that PIPs each have the potential to contribute substantial rates of POC export. The reported upper bound of global PIP estimates summed together is 8.7 Pg C yr⁻¹, which is comparable to the BGP export flux (Supplementary Table 1). This comprises 1.1–2.1 Pg C yr⁻¹ for the large-scale (and mesoscale) physical pumps (which also includes DOC^{22,23}), and 0.25–1.0, 0.9–3.6 and −0.09–2.0 Pg C yr⁻¹ from the lipid seasonal, mesopelagic migration, and eddy-subduction pumps, respectively (Fig. 2c). Thus, the cumulative contribution of PIPs may be as much as around 40% of total particle export (that is, BGP + PIPs). This suggests a considerable potential to resolve the imbalances reported for mesopelagic carbon demand¹⁷ and between nutrient and carbon export budgets¹⁵, and to lessen the variability between model estimates of global carbon sequestration (Supplementary Table 1).

We estimated the sequestration timescales for each PIP based on the passage time from the injection depth to the surface in an observationally constrained ocean circulation model¹⁴. Particles injected at the depth of the wintertime mixed-layer by the large-scale physical pumps (mixed-layer and subduction) result in sequestration for 25–100 years, assuming that subduction occurs before re-entrainment the next winter. In turn, deeper injection by the eddy-subduction pump (up to 450 m), the mesopelagic migration pump (up to 600 m) and the seasonal lipid pump (up to 1,400 m) translates to sequestration timescales of up to 150, 250 and 500 years respectively (Fig. 2b). These timescales will increase if it is assumed that sinking rather than suspended particles are injected, as sinking particles remineralize deeper than the injection horizon (Supplementary Methods).

Given the wide-ranging estimates of carbon injection rate (Fig. 2c) and depth (Fig. 2b) for each PIP, oceanic carbon sequestration by these mechanisms cannot be estimated with precision (Fig. 2d). However, choosing central values from the reported ranges of each property enables a first-order comparison between PIPs and the BGP. The mesopelagic migration pump emerges as the most important PIP, potentially storing around 60% as much carbon as the BGP in the ocean interior if large, sinking particles (that is, faecal pellets) are injected. The carbon-storage potential of the seasonal lipid, eddy-subduction and large-scale subduction pumps are approximately 20%, 10% and 5% that of the BGP, respectively, assuming that each pump injects suspended particles. The small net value for the large-scale subduction pump is due to the offsetting of subduction by strong obduction (upward transport of water parcels) in the equatorial oceans³⁹. On the basis of these central values (Fig. 2d), it is likely that the reservoir of respired carbon in the ocean interior contributed by the PIPs approaches that contributed by the BGP, and may therefore help to close global-scale mesopelagic carbon budgets^{15,16}.

Tracer constraints on the fate of exported carbon

Oceanic carbon sequestration by the BGP and by wide-ranging biophysical mechanisms that inject biogenic particles to depth depend critically on the fate of exported carbon (Fig. 2). However, at present, tracing the remineralization of particles (regardless of their export pathway) as they settle and circulate through the global ocean remains a logistical challenge, owing to the difficulties of deep-water particle sampling. Recently, new methods have used 3D ocean data assimilation models to leverage geochemical ‘remineralization tracers’, including oxygen and nutrients. These tracers integrate particle remineralization signatures over long timescales, and their global distributions are characterized by orders-of-magnitude more observations than are available for particles^{16,31,73}. Two distinct approaches have been applied. The first diagnoses remineralization rates directly from phosphate accumulation along transport pathways in a circulation model, and reconstructs particulate flux profiles that are required to explain the global distribution of remineralized phosphate³¹. The second assimilates geochemical and satellite data into mechanistic biogeochemical models to optimize key particle flux parameters, yielding mechanistic insights while leveraging the observations less directly⁷³.

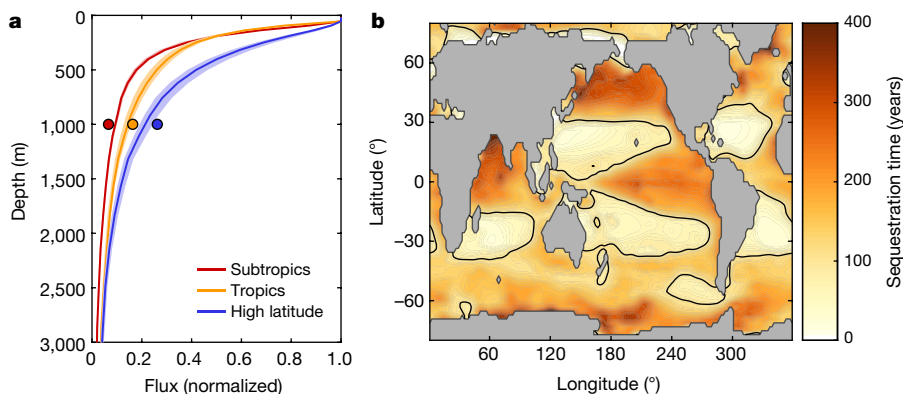


Fig. 3 | Fate of exported organic matter constrained in models from geochemical remineralization tracers. **a**, Organic matter flux over depth (normalized to flux at the base of the euphotic zone), averaged across subtropics, tropics and high latitude regions (as defined in ref. ³¹). Lines show flux profiles from a mechanistic model⁷³ that is optimized to match geochemical constraints (shading represents the range between 12 model configurations); circles represent the transfer efficiency diagnosed directly

Both approaches have yielded similar results and provide evidence for regional variability in particle flux attenuation, with the flux attenuating slowly at high latitudes and quickly in subtropical gyres; the tropics lie between these two extremes (Fig. 3a). These simulations reveal that carbon exported from high latitudes and tropical surface waters is sequestered longer in the interior of the oceans than is carbon exported in the oligotrophic gyres (Fig. 3b). This has important implications for feedbacks between the particle export and the global climate. Atmospheric P_{CO_2} is probably more sensitive to past changes in high-latitude export than has previously been recognized⁸, and the future expansion of subtropical habitats⁹ may result in less efficient (although not currently quantifiable) carbon sequestration in a warming world.

Regional variations in particle flux attenuation have largely been interpreted in terms of the balance between decomposition and sinking rates³². A likely explanation for the observed latitudinal pattern is the temperature-dependent metabolism of heterotrophs that are responsible for particle decomposition^{32,73}; however, variations in particle size and/or ballast are valid alternatives⁷³. There may also be a secondary effect of oxygen, as decomposition rates are slower in anoxic zones^{73,74} and even in hypoxic waters, due to the formation of anaerobic microenvironments in the particles⁷⁵.

To some degree, model-derived particle flux profiles may also reflect the relative magnitude of different export pathways (PIPs and BGP)—which vary in the injection depth and nature of particles they supply—because geochemical tracers integrate the effects of all export mechanisms. Deep injection by PIPs would result in slower flux attenuation over depth, whereas the injection of suspended particles that remineralize shallower in the water column would be diagnosed as rapid flux attenuation. Predicting future changes in ocean carbon sequestration will require a better understanding of the contribution of injection versus remineralization processes to the sequestration efficiency (Fig. 3b), given the different environmental sensitivity of these processes.

The need for prediction motivates the development of new techniques to distinguish between particle flux associated with the BGP and with each PIP. Particle stoichiometry (that is, carbon: nitrogen:phosphorus) may be central to identifying particular mechanisms that decouple their export. For example, diagnosing oxygen consumption between 500–1,500 m (the depth of zooplankton hibernation) without concomitant nutrient accumulation would point to carbon export by the seasonal lipid pump³⁰. Alternatively, diagnosing seasonal cycles of nutrient accumulation and oxygen-consumption rates would help to distinguish between the

from nutrient accumulation in an ocean circulation model³¹.

b, Sequestration time of exported carbon (replotted from data originally published in ref. ³¹). The spatial pattern reflects both variability in the particle flux attenuation (see a) and patterns of large-scale circulation. The thin black lines separate regions of efficient (>100 years) and inefficient (<100 years) carbon sequestration.

remineralization of particles exported by physical pumps and particle settling, both of which should exhibit distinct seasonality (Fig. 2a). This approach may soon be possible, given the burgeoning spatial and temporal resolution of tracer data provided by BGC-Argo floats (Supplementary Fig. 1) as well as emerging float sensor technology (Supplementary Table 2).

Extrapolation: towards a 4D view of particle export

To improve the accuracy of the initial estimates of the magnitude of carbon sequestration presented in Fig. 2d, the development of a 4D picture of particle flux and storage in the interior of the oceans would be required. It is clear from our development of PIP mechanisms that multiple scales—from sub-mesoscale to basin—must be accommodated if PIPs are to be assembled, first spatially and then temporally, into a complete 4D picture. Again, lessons on how to approach such upscaling can be gleaned from BGP research, which has imprinted both spatial and seasonal signatures (satellite remote-sensing and modelling)²⁶ onto short-term (days and weeks) observations taken at specific sites (Box 1). The timescales and lifetimes of features such as submesoscale eddies and fronts or seasonal mesopelagic export signatures (Fig. 2a) must be characterized to define the temporal footprint of each PIP and move towards a 4D viewpoint. This framework must be linked to the seasonality of pelagic particle production to assess whether a large portion of these upper ocean particles are subducted during a distinctive time period (Fig. 2a). For example, it is well established that submesoscale dynamics are strongly seasonal, with stronger and deeper penetration during winter than during summer⁷⁶.

Some published approaches towards extrapolating PIPs globally, and to climatological timescales, are outlined in Supplementary Table 1. The identification of the specific drivers of each PIP mechanism should help to improve modelling and hence extrapolation. We advocate the utility of explicitly incorporating the different PIP mechanisms into predictive, mechanistic models as a means to extrapolate PIPs into 4D. In the case of the extrapolation of the submesoscale eddy-subduction PIP, increasing the model grid resolution to incorporate these features is necessary and is now achievable in regional configurations^{77,78}. By contrast, other physically mediated PIPs—such as the large-scale subduction and mixed-layer pumps—are already represented in global models, and so their extrapolation requires the development of diagnostics to enable the simulated POC and DOC distributions to be better evaluated against observations²³. At present, the biologically mediated PIPs are not incorporated into state-of-the-art biogeochemical models^{9,14,31,77,78}. Although simulating animal behaviour at the global scale remains a grand challenge in ocean modelling, simple parameterizations have

been developed to predict the geochemical effect of the mesopelagic-migrant pump⁶, which might be further expanded to incorporate hibernation and therefore the seasonal lipid pump. It is only very recently that diel vertical migration has been incorporated for the first time in a global ocean general-circulation model and used to estimate the associated flux of carbon at the global scale⁷⁹. Although promising, this approach remains challenging because it is based on a computationally intensive, end-to-end ecosystem model, involving the interaction of all trophic levels from phytoplankton to top predators.

Transforming our view of ocean carbon export

Our synthesis of physically and biologically mediated PIPs reveals that they are directly transporting substantial stocks of biogenic particles to depth, of a cumulative magnitude that may be equivalent to the carbon storage of the BGP. The potential of PIPs to make a major contribution to the ocean carbon budget must now be explored in more detail, commencing with those PIPs that are most likely to contribute to carbon sequestration. The development of estimates of particle export, injection depth and circulation timescales reveals that the mesopelagic-migrant pump has the greatest potential to contribute to carbon sequestration, followed by the seasonal lipid pump and the various physical pumps (Fig. 2d). In the case of the seasonal lipid pump, its geographical realm of influence is already established³⁰, whereas less is known about the regional contributions of the mesopelagic-migrant pump⁵.

For all PIPs, the most pressing research issue—needed to address double-accounting issues and improve estimates of carbon sequestration—is to better understand the mechanisms of particle transformations^{17,65–68} (Fig. 1) within a 4D framework. Specifically, the fate of exported particles between their injection depth and the permanent pycnocline remains poorly constrained. A first step will be improved particle characterization, in particular the ability to distinguish zooplankton from other particle types, and to construct aggregate particle size distribution (PSD) profiles through the development and application of new sensors (Supplementary Table 2). Future developments in acoustic and imaging technologies⁸⁰ must be deployed on a range of platforms from ships (that is, to provide data for sensor calibration purposes) to an array of long-lived (that is, years), geographically diverse BGC-Argo floats. These developments towards the improvement of particle characterization will reduce the likelihood of double-accounting. Moreover, the alignment of BGC-Argo deployments (Box 1) with the characteristic space- and timescales of PIPs will enable better quantification of the role of patchiness in driving observed local and regional hotspots in biological PIPs^{30,54,56}. In time, following the development and testing of a Coastal-Argo platform, they can also be deployed to coastal and shelf seas to explore the role of PIPs in these regions (Supplementary Table 2).

The way forward in refining estimates of the contribution of PIPs in closing the ocean carbon budget^{15–17} also requires leveraging advancements in ocean biogeochemical modelling. Models are valuable testbeds on which to investigate the sensitivity of carbon storage mechanisms and guide future observations. For example, model sensitivity analyses point to the pivotal role of PSD in determining the fate of exported carbon^{31,73}; however, the processes that determine the PSD of exported particles and its evolution over depth remain only crudely parameterized. The development of robust models of particle transformations between multiple size classes, and incorporating them into general circulation models, will enable us to trace the fate of particles injected by different PIPs and dissect their contribution to carbon sequestration, while avoiding double-accounting issues.

Inverse methods that can assimilate PSD fields from new BGC-Argo technologies⁸¹ will enable models to ‘learn’ from the data, further refining them to better reflect the real ocean. Furthermore, downscaling of physical models is essential in order to simulate the locations of PIP injections—to support observational programmes such as high-resolution altimetry⁸²—and to integrate detailed particle transformations into submesoscale models⁸³.

To transform the comprehension of particle export from one- to three- and eventually four dimensions, it will be necessary to use machine-learning methods⁸⁴ that can be trained to predict unknown variables—such as particle flux—from better-sampled variables. Approaches such as artificial neural networks⁸⁵ will enable and enhance the upscaling of local and/or regional datasets that is needed to provide more robust extrapolation^{86,87} to depth, both regionally and annually, for each PIP. This upscaling is essential to refine estimates of the contribution of each PIP to carbon sequestration. BGC-Argo datasets will also eventually be combined with new satellite products, such as hyperspectrally resolved ocean colour observations of biology processes⁸⁸ and submesoscale characterization of sea level using high-resolution altimetry⁸².

Satellite and water-column remote-sensing, along with targeted process studies, will yield expansive datasets that can be assimilated into regional and global models of ever-increasing realism and resolution. Together, these approaches will lead towards a robust, four-dimensional view of carbon sequestration by the ocean’s multi-faceted biophysical particle pumps.

Online content

Any methods, additional references, Nature Research reporting summaries, source data, statements of data availability and associated accession codes are available at <https://doi.org/10.1038/s41586-019-1098-2>.

Received: 5 April 2018; Accepted: 1 February 2019;

Published online 17 April 2019.

1. Sarmiento, J. L. & Gruber, N. *Ocean Biogeochemical Dynamics* Ch. 8 (Princeton Univ. Press, Princeton, 2006).
2. Volk, T. & Hoffert, M. in *The Carbon Cycle and Atmospheric CO₂: Natural Variations Archean to Present* Vol. 32 (eds Sundquist, E. T. & Broecker, W. S.) 99–110 (American Geophysical Union, Washington, DC, 1985).
3. McKinley, G. A. et al. Timescales for detection of trends in the ocean carbon sink. *Nature* **530**, 469–472 (2016).
4. Buesseler, K. O. et al. Revisiting carbon flux through the ocean’s twilight zone. *Science* **316**, 567–570 (2007).
5. Irigoien, X. et al. Large mesopelagic fishes biomass and trophic efficiency in the open ocean. *Nat. Commun.* **5**, 3271 (2014).
6. Maier-Reimer, E., Mikolajewicz, U. & Winguth, A. Future ocean uptake of CO₂: interaction between ocean circulation and biology. *Clim. Dyn.* **12**, 711–722 (1996).
7. Bopp, L. et al. Multiple stressors of ocean ecosystems in the 21st century: Projections with CMIP5 models. *Biogeosciences* **10**, 6225–6245 (2013).
8. Martínez-García, A. et al. Iron fertilization of the Subantarctic ocean during the last ice age. *Science* **343**, 1347–1350 (2014).
9. Moore, J. K. et al. Sustained climate warming drives declining marine biological productivity. *Science* **359**, 1139–1143 (2018).
10. Bernadello, R. et al. Response of the ocean natural carbon storage to projected twenty-first-century climate change. *J. Clim.* **27**, 2033–2053 (2015).
11. Boyd, P. W. & Trull, T. W. Understanding the export of biogenic particles in oceanic waters: Is there consensus? *Prog. Oceanogr.* **72**, 276–312 (2007).
12. Buesseler, K. O. & Boyd, P. W. Shedding light on processes that control particle export and flux attenuation in the twilight zone of the open ocean. *Limnol. Oceanogr.* **54**, 1210–1232 (2009).
13. Martin, J., Knauer, G., Karl, D. & Broenkow, W. VERTEX: Carbon cycling in the northeast Pacific. *Deep Sea Res. Part A* **34**, 267–285 (1987).
14. DeVries, T., Primeau, F. & Deutsch, C. The sequestration efficiency of the biological pump. *Geophys. Res. Lett.* **39**, (2012).
15. Emerson, S. Annual net community production and the biological carbon flux in the ocean. *Glob. Biogeochem. Cycles* **28**, 14–28 (2014).
16. Schlitzer, R. Carbon export fluxes in the Southern Ocean: results from inverse modeling and comparison with satellite based estimates. *Deep Sea Res. Part II Top. Stud. Oceanogr.* **49**, 1623–1644 (2002).
17. Burd, A. B. et al. Assessing the apparent imbalance between geochemical and biochemical indicators of meso- and bathypelagic biological activity: What the @#\$! is wrong with present calculations of carbon budgets? *Deep Sea Res. Part II Top. Stud. Oceanogr.* **57**, 1557–1571 (2010).
18. Giering, S. L. et al. Reconciliation of the carbon budget in the ocean’s twilight zone. *Nature* **507**, 480–483 (2014).
19. Steinberg, D. K. et al. Bacterial vs. zooplankton control of sinking particle flux in the ocean’s twilight zone. *Limnol. Oceanogr.* **53**, 1327–1338 (2008).
20. Reinharter, T. et al. Prokaryotic respiration and production in the meso- and bathypelagic realm of the eastern and western North Atlantic basin. *Limnol. Oceanogr.* **51**, 1262–1273 (2006).

This paper reviewed the (lack of) progress on constraining mesopelagic carbon budgets, and advocated new approaches to tackle this issue.

This paper presented one of the few balanced mesopelagic carbon budgets by assessing community respiration versus carbon demand.

21. Boyd, P. W., McDonnell, A. & Valdez, J. RESPIRE: An in situ particle interceptor to conduct particle remineralization and microbial dynamics studies in the oceans' twilight zone. *Limnol. Oceanogr. Meth.* **13**, 494–508 (2015).

22. Hansell, D. A., Carlson, C. A., Repeta, D. J. & Schlitzer, R. Dissolved organic matter in the ocean. *Oceanography (Wash. DC)* **22**, 202–211 (2009).

23. Lévy, M. et al. Physical pathways for carbon transfers between the surface mixed layer and the ocean interior. *Glob. Biogeochem. Cycles* **27**, 1001–1012 (2013).

24. Henson, S. A., Yool, A. & Sanders, R. Variability in efficiency of particulate organic carbon export: A model study. *Geophys. Res. Lett.* **29**, 33–45 (2015).

25. Aumont, O. et al. Variable reactivity of particulate organic matter in a global ocean biogeochemical model. *Biogeosciences* **14**, 2321–2341 (2017).

26. Siegel, D. A. et al. Global assessment of ocean carbon export by combining satellite observations and food-web models. *Glob. Biogeochem. Cycles* **28**, 181–196 (2014).

27. Stukel, M. R., Song, H., Goericke, R. & Miller, A. J. The role of subduction and gravitational sinking in particle export, carbon sequestration, and the remineralization length scale in the California Current Ecosystem. *Limnol. Oceanogr.* **63**, 363–383 (2017).

28. Omand, M. M. et al. Eddy-driven subduction exports particulate organic carbon from the spring bloom. *Science* **348**, 222–225 (2015). **This paper quantified the eddy-subduction pump by using an array of gliders in the North Atlantic during the spring bloom.**

29. Dall'Olmo, G., Dingle, J., Polimene, L., Brewin, R. J. W. & Claustre, H. Substantial energy input to the mesopelagic ecosystem from the seasonal mixed-layer pump. *Nat. Geosci.* **9**, 820–823 (2016). **This paper quantified the mixed-layer pump across large regions of the high latitude ocean.**

30. Jónasdóttir, S. H., Visser, A. W., Richardson, K. & Heath, M. R. Seasonal copepod lipid pump promotes carbon sequestration in the deep North Atlantic. *Proc. Natl. Acad. Sci. USA* **112**, 12122–12126 (2015). **This paper provided the first detailed quantification of the seasonal lipid pump.**

31. Weber, T., Cram, J. A., Leung, S. W., DeVries, T. & Deutsch, C. Deep ocean nutrients imply large latitudinal variation in particle transfer efficiency. *Proc. Natl. Acad. Sci. USA* **113**, 8606–8611 (2016).

32. Marsay, C. M. et al. Attenuation of sinking particulate organic carbon flux through the mesopelagic ocean. *Proc. Natl. Acad. Sci. USA* **112**, 1089–1094 (2015).

33. Giering, S. L. C. et al. Particle flux in the oceans: Challenging the steady state assumption. *Glob. Biogeochem. Cycles* **31**, 159–171 (2017).

34. Jiao, N. et al. Microbial production of recalcitrant dissolved organic matter: long-term carbon storage in the global ocean. *Nat. Rev. Microbiol.* **8**, 593–599 (2010).

35. Swan, B. K. et al. Potential for chemolithoautotrophy among ubiquitous bacteria lineages in the dark ocean. *Science* **333**, 1296–1300 (2011).

36. Bishop, J. K. B., Conte, M. H., Wiebe, P. H., Roman, M. R. & Langdon, C. Particulate matter production and consumption in deep mixed layers: Observations in a warm-core ring. *Deep Sea Res. Part A* **33**, 1813–1841 (1986).

37. Dall'Olmo, G. & Mork, K. A. Carbon export by small particles in the Norwegian Sea. *Geophys. Res. Lett.* **41**, 2921–2927 (2014).

38. Cushman-Roisin, B. Subduction. In *Dynamics of the Oceanic Surface Mixed Layer*, Proc. 'Aha Huliko'a, Hawaiian Winter Workshop (eds Muller, P. & Henderson, D.) 181–196 (Hawaii Institute of Geophysics, 1987).

39. Marshall, J., Nurser, A. & Williams, R. Inferring the subduction rate and period over the North Atlantic. *J. Phys. Oceanogr.* **23**, 1315–1329 (1993).

40. Liu, L. L. & Huang, R. X. The global subduction/obduction rates: Their interannual and decadal variability. *J. Clim.* **25**, 1096–1115 (2012).

41. Pollard, R. T. & Regier, L. Large variations in potential vorticity at small spatial scales in the upper ocean. *Nature* **348**, 227–229 (1990).

42. Nurser, A. & Zhang, J. Eddy-induced mixed layer shallowing and mixed layer/thermocline exchange. *J. Geophys. Res. Oceans* **105**, 21851–21868 (2000).

43. Niewiadomska, K., Claustre, H., Prieur, L. & D'Ortenzio, F. Submesoscale physical-biogeochemical coupling across the Ligurian Current (northwestern Mediterranean) using a bio-optical glider. *Limnol. Oceanogr.* **53**, 2210–2225 (2008).

44. Estapa, M. L. et al. Decoupling of net community and export production on submesoscales in the Sargasso Sea. *Glob. Biogeochem. Cycles* **29**, 1266–1282 (2015).

45. Lévy, M., Klein, P. & Treguer, A.-M. Impacts of sub-mesoscale physics on phytoplankton production and subduction. *J. Mar. Res.* **59**, 535–565 (2001).

46. Nagai, T., Gruber, N., Frenzel, H., Lachkar, Z., McWilliams, J. C. & Plattner, G.-K. Dominant role of eddies and filaments in the offshore transport of carbon and nutrients in the California Current System. *J. Geophys. Res. Oceans* **120**, 5318–5341 (2015).

47. Karleskind, P., Lévy, M. & Memery, L. Modifications of mode water properties by sub-mesoscales in a bio-physical model of the Northeast Atlantic. *Ocean Model.* **39**, 47–60 (2011).

48. Karleskind, P., Lévy, M. & Memery, L. Subduction of carbon, nitrogen, and oxygen in the northeast Atlantic. *J. Geophys. Res. Oceans* **116**, C02025 (2011).

49. Stukel, M. R. et al. Mesoscale ocean fronts enhance carbon export due to gravitational sinking and subduction. *Proc. Natl. Acad. Sci. USA* **114**, 1252–1257 (2017). **This paper compared the magnitude of export fluxes from the biological pump and the eddy-subduction pump.**

50. Vinogradov, M. E. Some problems of vertical distribution of meso- and macroplankton in the ocean. *Adv. Mar. Biol.* **32**, 1–92 (1997).

51. Steinberg, D. K. & Landry, M. R. Zooplankton and the ocean carbon cycle. *Ann. Rev. Mar. Sci.* **9**, 413–444 (2017).

52. Bianchi, D., Stock, C., Galbraith, E. D. & Sarmiento, J. L. Diel vertical migration: ecological controls and impacts on the biological pump in a one-dimensional ocean model. *Glob. Biogeochem. Cycles* **27**, 478–491 (2013).

53. Bianchi, D., Galbraith, E. D., Carozza, D. A., Mislan, K. A. S. & Stock, C. A. Intensification of open-ocean oxygen depletion by vertically migrating animals. *Nat. Geosci.* **6**, 545–548 (2013). **This paper used global Acoustic Doppler Current Profiler observations to constrain the Mesopelagic migration pump.**

54. Davison, P. C., Checkley, D. M., Jr, Koslow, J. A. & Barlow, J. Carbon export mediated by mesopelagic fishes in the northeast Pacific Ocean. *Prog. Oceanogr.* **116**, 14–30 (2013). **This paper used trawl surveys and metabolic modelling to assess the export fluxes mediated by mesopelagic fishes.**

55. Childress, J. J., Taylor, S. M., Cailliet, G. M. & Price, M. H. Patterns of growth, energy utilization and reproduction in some meso- and bathypelagic fishes off Southern California. *Mar. Biol.* **61**, 27–40 (1980).

56. Klevjer, T. A. et al. Large scale patterns in vertical distribution and behaviour of mesopelagic scattering layers. *Sci. Rep.* **6**, 19873 (2016).

57. Bradford-Grieve, J. M., Nodder, S. D., Jillet, J. B., Currie, K. & Lassey, K. R. Potential contribution that the copepod *Neocalanus tonsus* makes to downward carbon flux in the Southern Ocean. *J. Plankton Res.* **23**, 963–975 (2001).

58. Kobari, T. et al. Impacts of ontogenetically migrating copepods on downward carbon flux in the western subarctic Pacific Ocean. *Deep Sea Res. Part II Top. Stud. Oceanogr.* **55**, 1648–1660 (2008).

59. Dam, H. G., Miller, C. A. & Jonasdottir, S. H. The trophic role of mesozooplankton at 47°N, 20°W during the North Atlantic Bloom Experiment. *Deep Sea Res. Part II Top. Stud. Oceanogr.* **40**, 197–212 (1993).

60. Turner, J. T. Zooplankton fecal pellets, marine snow, phytodetritus and the ocean's biological pump. *Prog. Oceanogr.* **130**, 205–248 (2015).

61. Bishop, J. K. B. in *Productivity of the Ocean: Present and Past* (eds Berger W. H., Smetacek, V. S. & Wefer, G.) 117–137 (Wiley Interscience, New York, 1989).

62. McDonnell, A. M. P., Boyd, P. W. & Buesseler, K. O. Effects of sinking velocities and microbial respiration rates on the attenuation of particulate carbon fluxes through the mesopelagic zone. *Glob. Biogeochem. Cycles* **29**, 175–193 (2015).

63. Durkin, C. A., Estapa, M. L. & Buesseler, K. O. Observations of carbon export by small sinking particles in the upper mesopelagic. *Mar. Chem.* **175**, 72–81 (2015).

64. Cavan, E. L., Trimmer, M., Shelley, F. & Sanders, R. Remineralization of particulate organic carbon in an ocean oxygen minimum zone. *Nat. Commun.* **8**, 14847 (2017).

65. Alldredge, A. L. & Silver, M. W. Characteristics, dynamics and significance of marine snow. *Prog. Oceanogr.* **20**, 41–82 (1988).

66. Jackson, G. A. A model of the formation of marine algal flocs by physical coagulation processes. *Deep Sea Res. A* **37**, 1197–1211 (1990).

67. Kørboe, T. Formation and fate of marine snow: small-scale processes with large-scale implications. *Sci. Mar.* **65**, 57–71 (2001).

68. Iversen, M. H. & Ploug, H. Temperature effects on carbon-specific respiration rate and sinking velocity of diatom aggregates – potential implications for deep ocean export processes. *Biogeosciences* **10**, 4073–4085 (2013).

69. Ohman, M. D., Powell, R., Picheral, M. & Jensen, D. W. Mesozooplankton and particulate matter responses to a deep-water frontal system in the southern California Current System. *J. Plankton Res.* **34**, 815–827 (2012).

70. D'Asaro, E. A. et al. Ocean convergence and the dispersion of flotsam. *Proc. Natl. Acad. Sci.* **30**, 1162–1167 (2018).

71. Briggs, N. et al. High-resolution observations of aggregate flux during a sub-polar North Atlantic spring bloom. *Deep Sea Res. Part I Oceanogr. Res. Pap.* **58**, 1031–1039 (2011).

72. Stanley, R. H. R., McGillicuddy, D. J., Jr, Sandwith, Z. O. & Pleskow, H. M. Submesoscale hotspots of productivity and respiration: Insights from high resolution oxygen and fluorescence sections. *Deep Sea Res. Part I Oceanogr. Res. Pap.* **130**, 1–11 (2017).

73. DeVries, T. & Weber, T. The export and fate of organic matter in the ocean: New constraints from combining satellite and oceanographic tracer observations. *Glob. Biogeochem. Cycles* **31**, 535–555 (2017).

74. Cram, J. A., Weber, T., Leung, S. W., McDonnell, A. M. P., Liang, J.-H. & Deutsch, C. The role of particle size, ballast, temperature, and oxygen in the sinking flux to the deep sea. *Glob. Biogeochem. Cycles* **32**, 858–876 (2018).

75. Bianchi, D., Weber, T. S., Kiko, R. & Deutscher, C. Global niche of marine anaerobic metabolisms expanded by particle microenvironments. *Nat. Geosci.* **11**, 263–268 (2018).

76. Callies, J., Ferrari, R., Klymak, J. M. & Gula, J. Seasonality in submesoscale turbulence. *Nat. Commun.* **6**, 6862–6869 (2015).

77. Lévy, M. et al. Large-scale impacts of submesoscale dynamics on phytoplankton: Local and remote effects. *Ocean Model. (Oxf.)* **43–44**, 77–93 (2012).

78. Harrison, C. S., Long, M. C., Lovenduski, N. S. & Moore, J. K. Mesoscale effects on carbon export: A global perspective. *Glob. Biogeochem. Cycles* **32**, 680–703 (2018).

79. Aumont, O. et al. Evaluating the potential impacts of the diurnal vertical migration by marine organisms on marine biogeochemistry. *Glob. Biogeochem. Cycles* **32**, 1622–1643 (2018).

80. Picheral, M. et al. The Underwater Vision Profiler 5: An advanced instrument for high spatial resolution studies of particle size spectra and zooplankton. *Limnol. Oceanogr. Methods* **8**, (2010).

81. Johnson, K. Biogeochemical sensors for autonomous, Lagrangian platforms: Current status, future directions. *Autonomous and Lagrangian Platforms and Sensors ALPS II* <https://alps-ocean.us/agenda/> (2017).

82. Fu, L.-L. & Ubelmann, C. On the transition from profile altimeter to swath altimeter for observing global ocean surface topography. *J. Atmos. Ocean. Technol.* **31**, 560–568 (2014).

83. Resplandy, L. et al. How does dynamical spatial variability impact ^{234}Th -derived estimates of organic export? *Deep Sea Res. Part I Oceanogr. Res. Pap.* **68**, 24–45 (2012).

84. Castelvecchi, D. Can we open the black box of AI? *Nature* **538**, 20–23 (2016).

85. Sauzède, R. et al. A neural network-based method for merging ocean color and Argo data to extend surface bio-optical properties to depth: Retrieval of the particulate backscattering coefficient. *J. Geophys. Res. Oceans* **121**, 2552–2571 (2016).

86. Landschützer, P. et al. A neural network-based estimate of the seasonal to inter-annual variability of the Atlantic Ocean carbon sink. *Biogeosciences* **10**, 7793–7815 (2013).

87. Landschützer, P., Gruber, N., Bakker, D. C. E. & Schuster, U. Recent variability of the global ocean carbon sink. *Glob. Biogeochem. Cycles* **28**, 927–949 (2014).

88. Werdell, P. J. et al. An overview of approaches and challenges for retrieving marine inherent optical properties from ocean color remote sensing. *Prog. Oceanogr.* **160**, 186–212 (2018).

89. Boyd, P. W. et al. The evolution and termination of an iron-induced mesoscale bloom in the northeast subarctic Pacific Ocean. *Limnol. Oceanogr.* **50**, 1872–1886 (2005).

90. Ohman, M. D. & Romagnan, J.-B. Nonlinear effects of body size and optical attenuation on Diel Vertical Migration by zooplankton. *Limnol. Oceanogr.* **61**, 765–770 (2016).

91. Powell, J. R. & Ohman, M. D. Use of glider-class acoustic Doppler profilers for estimating zooplankton biomass. *J. Plankton Res.* **34**, 563–568 (2012).

92. Siegel, D. A. & Deuser, W. G. Trajectories of sinking particles in the Sargasso Sea: Modeling of statistical funnels above deep-ocean sediment traps. *Deep Sea Res. Part I Oceanogr. Res. Pap.* **44**, 1519–1541 (1997).

93. Siegel, D. A., Fields, E. & Buesseler, K. O. A bottom-up view of the biological pump: Modeling source funnels above ocean sediment traps. *Deep Sea Res. Part I Oceanogr. Res. Pap.* **55**, 108–127 (2008).

94. Llort, J. et al. Evaluating Southern Ocean carbon eddy-pump from biogeochemical Argo floats. *J. Geophys. Res. Oceans* (2018).

Acknowledgements P.W.B. was primarily supported by the Australian Research Council through a Laureate (FL160100131), and this research was also supported under the Australian Research Council's Special Research Initiative for Antarctic Gateway Partnership (project ID SR140300001). H.C. acknowledges the support of the European Research Council (remOcean project, grant agreement 246777) and of the Climate Initiative of the BNP Paribas foundation (SOCLIM project). M.L. was supported by CNES, by the ANR project SOBUMS (ANR-16-CE01-0014) and by the National Aeronautics and Space Administration (NASA) grant NNX16AR50G. D.A.S. acknowledges support from NASA as part of the Export Processes in the global Ocean from RemoTe Sensing (EXPORTS) field campaign, grant 80NSSC17K0692. T.W. was supported by National Science Foundation grant OCE-1635414.

Reviewer information *Nature* thanks Sarah Giering, Stephanie Henson, Gerhard Herndl, Andreas Oschlies and Paul Wassmann for their contribution to the peer review of this work.

Author contributions P.W.B. devised the concept and structure for this Review. All authors wrote the manuscript.

Competing interests The authors declare no competing interests.

Additional information

Supplementary information is available for this paper at <https://doi.org/10.1038/s41586-019-1098-2>.

Reprints and permissions information is available at <http://www.nature.com/reprints>.

Correspondence and requests for materials should be addressed to P.W.B.

Publisher's note: Springer Nature remains neutral with regard to jurisdictional claims in published maps and institutional affiliations.